Potential Energy Surfaces for LiH2 and Photochemical Reactions Li*+ H2↔ LiH+ H

ARTICLE *in* THE JOURNAL OF PHYSICAL CHEMISTRY A · DECEMBER 1999

Impact Factor: 2.69 · DOI: 10.1021/jp9921295

Potential Energy Surfaces for LiH_2 and Photochemical Reactions $Li^* + H_2 \leftrightarrow LiH + H$

Hyo Sug Lee and Yoon Sup Lee*

Department of Chemistry and Center for Molecular Science, Korea Advanced Institute of Science and Technology, Taejon 305-701, South Korea

Gwang-Hi Jeung*,†

Laboratoire Aimé Cotton (CNRS UPR3321), Bât. 505, and ASCI (CNRS UPR9029), Bât. 506, Université de Paris-Sud, 91405 Orsay, France

Received: June 24, 1999; In Final Form: August 23, 1999

Potential energy surfaces for the $Li^* + H_2 \rightarrow LiH + H$ and the reverse reactions are calculated using ab initio methods. Extensive configuration interactions have been done for a large number of collinear, C_{2v}, and C_s geometrical forms using a large basis set to describe the 2s−3d atomic states of the lithium atom and the neutral and anionic hydrogen molecule. The Li(3s) channel has a small activation barrier and leads to a stable intermediate, $4\ ^2A'\ (LiH_2)^*$, but a diabatic coupling between the 3 and $4\ ^2A'$ surfaces would preferentially lead to a nonreactive inelastic collision producing Li(2p). The Li(2p) channel leads to one entirely repulsive potential surface ($3\ ^2A'$) and two attractive potential surfaces ($2\ ^2A'$ and $1\ ^2A''$) resulting in two stable intermediates. The Li(2p) atoms with enough collision energy to overcome the endothermicity of 1624 cm^{-1} can lead to the reaction producing LiH. Those three excited intermediate complexes are bent (planar) and not linear. The charge transfer from the metal atom to the hydrogen molecule does not occur in the course of the collision but much later, when one hydrogen atom breaks away, implying that the harpooning model does not apply to this case. The reverse reaction $LiH + H \rightarrow Li + H_2$ can produce (i) the high-energy Li(2s) directly, (ii) the thermal Li(2p), and (iii) the thermal Li(2s) accompanied with a chemiluminescence. The $2\ ^2A'$ intermediate may play an important role in the reverse reaction, too.

I. Introduction

The collision between an alkali atom and a hydrogen molecule resulting in an inelastic scattering or a reactive substitution is one of the simplest three-body problems. The nuclear motion involves three degrees of freedom in a constant rotational frame of reference and only three valence electrons participate actively in this reaction, which facilitates experimental and theoretical studies. Since a spectacular laser-snow observation on the $Cs^* + H_2$ by Tam et al.,[1] many spectroscopic and reaction dynamic studies for the alkali atom and hydrogen molecule have been performed.

From the experimental point of view, the use of tunable lasers has brought a skipping progress in understanding the photochemical reactions. The electronic excitation of the reactant by lasers is a versatile way of both surmounting a large endoergic reaction barrier and selecting the initial electronic state. Nuclear states can be carefully chosen with the molecular jet technique or by regulating temperature and pressure of the reaction chamber. Use of tunable lasers also has allowed characterization of the state of reaction products by the laser induced-fluorescence spectroscopy or the resonance-enhanced multiphoton ionization. In this way, one can determine very precisely the final state distribution or a time-averaged statistical ensemble as a function of the initial state distribution.

The major problem of the $A^* + H_2 \rightarrow AH + H$ reaction, where A is the alkali atom, lies in connecting the final state to the initial state, or in finding a reaction mechanism. During the time interval between the excitation of the metal atom to the observation of the product, (i) the reactant might have undergone a single or a multiple collision, (ii) there might be a temporarily stable intermediate, $(AH_2)^*$, (iii) the nuclear kinetic energy might have been partially converted to vibration and rotation energies, (iv) the electronic state could have undergone several transitions (or potential energy crossings), (v) the hydrogen molecule might have been vibrationally excited, and (vi) a fraction of the energy could have been carried away through radiation. Combination of those factors makes the chronological reconstruction of the reaction a formidable task. The experimental findings should be interpreted in such a way as to give a coherent and plausible model. Since the present-state quantum chemical calculation can produce sufficiently reliable data for these systems, a careful look at the potential surfaces and the nature of the electronic wave functions can help to guess the likely reaction mechanism and to estimate the reaction rate.

Among the reactions $A^* + H_2 \rightarrow AH + H$, the simplest case is the one involving the lithium atom

$$Li(\alpha) + H_2(\nu,J) \rightarrow LiH(\nu'',J'') + H(\xi) \qquad (1)$$

where α is the electronic and translational quantum state and ξ is a translational quantum state. The endoergicity of this reaction for the ground-to-ground-state energy difference is the smallest in comparison with the reactions involving other alkali atoms, Na, K, Rb, and Cs. One should also consider the nonreactive elastic and inelastic collisions

$$Li(\alpha) + H_2 \rightarrow Li(\beta) + H_2 \qquad (2)$$

† E-mail: jeung@asci.fr. Fax: +33-169358406.

10.1021/jp9921295 CCC: $18.00
Published on Web 11/19/1999

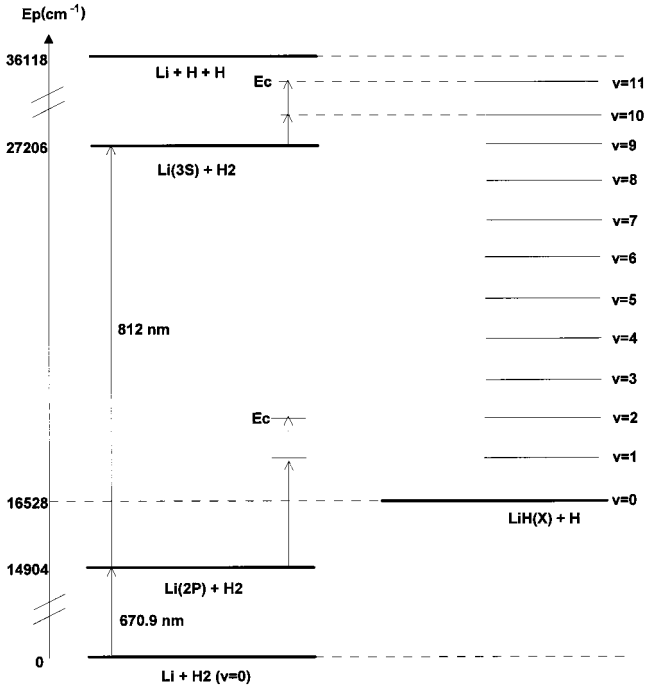

Figure 1. Energy diagram for the Li + H_2 and LiH + H.

where α and β represent the electronic and translational quantum states. (Here the rovibrational states of hydrogen molecule can also change.)

The concentration of the LiH molecule in the early universe is a key question to understand the creation of the primordial molecules. The reverse reaction to (1)

$$\mathrm{LiH} + \mathrm{H} \rightarrow \mathrm{Li} + \mathrm{H_2} \qquad (3)$$

which is supposed to be efficient, has been known to play an important role in the destruction of the LiH molecule.[2] However, the reaction rate of this reverse reaction is not well-known. The corresponding elastic and inelastic collisions would be

$$\mathrm{LiH}(\gamma) + \mathrm{H} \rightarrow \mathrm{LiH}(\delta) + \mathrm{H} \qquad (4)$$

where γ and δ represent the rovibrational quantum numbers.

In this work, we present an ab initio quantum chemical study for the reactions 1−3. The aim of this work is to get a bird's eye view for the potential energy surfaces (PESs), the nature of the electronic wave functions, and the transition properties involved in these reactions, so that we could predict the essential characteristics of these reactions. As only three valence electrons and two core electrons are involved in this system, the state of the art technique in ab initio calculations can produce a high-quality result. Rossi and Pascale[3] reported a semiempirical effective core potential calculation for the interaction between the alkali atoms and the hydrogen molecule where the internuclear distance of the hydrogen molecule was kept constant at 1.4 bohr. Martinez[4] has reported a quasi classical simulation for the Li(2p) + H_2 collision dynamics near the C_{2v} diabatic coupling region using the PESs calculated with an effective core potential and a double-ζ basis.

The energetics involved in the reaction 1 is as follows (see Figure 1). As the $v = 0$ bond energy (D_0) of H_2 is 4.478 eV and that of LiH is 2.429 eV,[5] this reaction is endoergic by 2.049 eV (16 528 cm^{-1}). The reaction cannot occur for the initial state of lithium in the 2p state (14 905 cm^{-1} over the 2s) except when the reactants collide with a high kinetic energy (higher than the difference energy of 0.201 eV). With the initial lithium state of 3s (27 206 cm^{-1} over the 2s), 3p (30 925 cm^{-1} over the 2s), or 3d state (31 283 cm^{-1} over the 2s),[6] the reaction is exoergic by 1.324, 1.785, or 1.829 eV, respectively, assuming zero kinetic (Li, H_2) and rovibrational (H_2) energies for the reactants. This large excess energy could be transferred to the rovibrational (v',J') energy of the LiH_2 system. This energy can then be transformed to the kinetic and rovibrational (v'',J'') energies of H and LiH (which may result in v'' up to 9), if the reaction takes place, and also to the fluorescent (i.e., involving the electronic state transition) photon energy. This is quite different from the Cs*+ H_2 → CsH + H case where the excess energy is only 9 cm^{-1} (Cs $7p_{1/2}$). It may be inferred that the intramolecular energy transfer would play an important role in the Li*+ H_2 → LiH + H reaction.

TABLE 1: Spectroscopic Data for Li, H_2, and LiH (in cm^{-1} and pm)

		calculated	experimental
Li	IP	43441	43487[a]
	ΔE (3p←2s)	30932	30925[a]
	ΔE (3s←2s)	27201	27206[a]
	ΔE (2p←2s)	14914	14904[a]
H_2	R_e	74.3	74.144[b]
	D_e	37868	37991[b]
	D_0	35687	36118.06[c]
	ω_e	4416	4401.21[b]
	$\omega_e x_e$	121.4	121.34[b]
	B_e	60.46	60.853[b]
LiH	R_e	160	159.5584[d]
	D_e	19705	20287.7[d]
	D_0	19011	19589.8[d]
	ω_e	1399	1405.1−1406.2[d]
	$\omega_e x_e$	23.67	22.68−23.55[d]
	B_e	7.471	7.5131−7.5143[d]

[a] Reference 6. [b] Reference 5. [c] Reference 37. [d] Reference 38.

II. Method of Computation

Our basis set for the lithium and hydrogen atoms is made as follows. For the lithium atom, all-electron (12s8p5d3f) Gaussian type orbitals (GTOs) were contracted to [9s8p5d3f] atomic basis functions (ABFs) to optimally describe the 2s, 2p, 3s, 3p, and 3d atomic states. The 1f GTO with the exponent 0.035 in this basis was determined to have the lowest energy for the ground state at a compact geometry (small internuclear distances). This was then split into 3f GTOs. The ground state of the lithium atom calculated in the Hartree−Fock (HF) method gave the total energy of −7.432 57 hartrees, which is close to the HF limit value, −7.432 73.[7] The atomic transition energies calculated with valence−core configuration interaction (CI) are in excellent agreement with the experimental data (see Table 1).

For the hydrogen atom, 5s GTOs reported before[8] among which the most diffuse GTO was determined for H^-, were contracted to 4s ABFs. The restricted HF energy of the hydrogen atom calculated with this basis is −0.499 354 hartree (au). The 1p GTO with the exponent 1.1 determined for the hydrogen molecule with CI and the 1p GTO with the exponent 0.2 determined for the hydrogen anion atom with CI were augmented by adding an intermediate 1p GTO with the exponent 0.47. The final set for hydrogen is (5s3p) → (4s3p). The electron affinity of the hydrogen atom calculated with this basis is 0.68

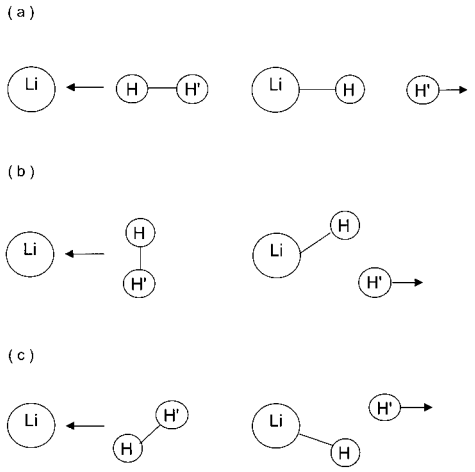

Figure 2. Geometrical types for the Li + H_2 and LiH + H studied in this work: (a) collinear ($C_{\infty v}$), (b) perpendicular (C_{2v}), and (c) oblique (C_s) cases.

eV, which is slightly smaller than the experimental value, 0.75 eV.[9] The remaining error of the electron affinity can make the LiH part of the potential energy surfaces slightly lower than our calculated values.

For the molecular calculations, the MOLCAS[10] and MOLPRO[11] programs were used. The three valence electrons were distributed in a set (active space) of molecular orbitals (MOs) made from the 2s, 2p, 3s, 3p, and 3d atomic orbitals (AOs) of lithium atom and two 1s AOs of the two hydrogen atoms in complete active space self-consistent field (CASSCF) calculations. The MOs were optimized for the average of all states made from this active space for each given symmetry species. Then multireference singles and doubles configuration interactions (MRCIs) were done upon the CAS-MOs. In the MRCI, the same active space as in the CASSCF was used, and no virtual MOs were discarded. Furthermore, two core electrons corresponding to the Li ($1s^2$) were allowed to do all possible single excitations, thus including the valence−core correlation effect. Inclusion of the core−core correlation does not change the relative energies significantly. This computational method is expected to give a highly accurate solution for the LiH_2. The dipole moments were calculated with the MRCI wave functions. The transition dipole moments were calculated with the CASSCF wave functions. Table 1 also shows our calculated spectroscopic constants for the H_2 and LiH molecules. Comparison with the experimental data indicates a good accuracy of our calculation.

Three geometric parameters, e.g., R(Li−H), R(H−H′), and R(Li−H′), are necessary to describe the PESs in a constantly rotating frame of reference. A large number of geometrical figures are possible. However, surveying a limited number of cases can show the general shape of PESs. The same set of PESs for LiH_2 can be used for both the reactions 1−4, as they only differ by the starting and ending directions. First, we have analyzed three types of Li + H_2 or LiH + H geometrical points (see Figure 2). The three Li + H_2 approaches can be named collinear (Li atom and the H_2 molecule forming a $C_{\infty v}$ point group symmetry), perpendicular (C_{2v}), and oblique (C_s) where the molecular axis of the hydrogen makes an angle of around $\pi/4$ (45°) with respect to the translational velocity of the lithium atom. For the LiH + H channel, the interatomic distances, R(Li−H), R(H−H′), and R(Li−H′), are varied in such a way that the center of mass remains fixed in each of the three geometrical types. Each of the three LiH + H geometrical types ($C_{\infty v}$, C_{2v}, C_s) and the corresponding Li + H_2 geometrical type can be described in the same constantly rotating frame of reference. For the calculation of the center of the mass, we have used the ^{7}Li isotope in this work. However, the potential energy is invariant upon isotope substitution within the Born−Oppenheimer approximation. One can imagine many other hypothetical reaction coordinates (i.e., a series of consecutive geometries connecting the starting point and the end point), but our choice happens to give no potential barrier for the exit channel (LiH + H) as can be seen later. As the PESs in this work are in fact hypersurfaces in four dimensions, this classification of three types of molecular geometry is not only a convenient way to represent the PES in figure but also very useful in analyzing the reaction dynamics. Second, we have calculated many other geometrical points which can be considered as in-between cases. The potential energies, the dipole moments, the transition dipole moments, and other raw data used in this work are available upon request.

Mizutani et al.[12] have calculated a large area of the PESs for the Li(2s) and Li(2p) with a CASSCF method. However, the basis set used in that work, a minimal basis, might be too inflexible to describe the polarization and the correlation effect. Clarke et al.[13] have calculated the ground state PES limited to the collinear case, which might be incomplete to understand the interaction between the lithium atom and the hydrogen molecule.

III. Results

The PES sections corresponding to the collinear cases are drawn in Figure 3a. The PES sections corresponding to the perpendicular Li + H_2 reactant case and the corresponding Li + H center of mass conserving product departure case are drawn in Figure 3b. The PES sections for the oblique cases are drawn in Figure 3c. These figures show the essential feature of the reactive or nonreactive collisions. In this work, the collisions involving Li(2s), Li(2p), and Li(3s) with the hydrogen molecules will be discussed.

The ground state PES is repulsive as the distance between the lithium atom and the hydrogen molecule becomes smaller. So the ground state adiabatic PES is an uphill (or downhill depending upon the colliding or recoiling point of view, respectively) valley. The long-range van der Waals interaction is not strong enough to make a vibrationally stable potential well, i.e., the ground state is unstable. The Li + H_2 collision is uninteresting in usual thermal conditions: only nonreactive elastic and inelastic scattering can result.

(a) Li(3s) + H_2. The Li(3s) initial state leads to an attractive potential well resulting in a stable $(LiH_2)^*$ complex. The lowest energy of this state, 4 ^{2}A′, corresponds to a C_s geometry with the internuclear distance between the lithium atom and the nearer hydrogen atom (H), R(Li−H), being 175 pm, the internuclear distance between the lithium atom and the farther hydrogen atom (H′), R(Li−H′), being 229 pm, and the distance between the two hydrogen atoms, R(H−H′), being 78 pm (see Table 2). The C_{2v} geometry has the lowest potential energy about 700 cm^{-1} higher than the minimum C_s geometry and the collinear ($C_{\infty v}$) geometry about 800 cm^{-1} higher.

As the 4 ^{2}A′ state is attractive, the zero-point vibration and the low level rotation ($J = 0$ or 1 in usual supersonic molecular beam experiments) of the hydrogen molecule when the collision partners are far apart change to the internal vibrations as the complex is formed. This internal vibration keeps this excited complex (or exciplex) dynamically stable. Without a partial transformation of the collision energy into the vibrational excitation, only the elastic scattering would result. The lifetime

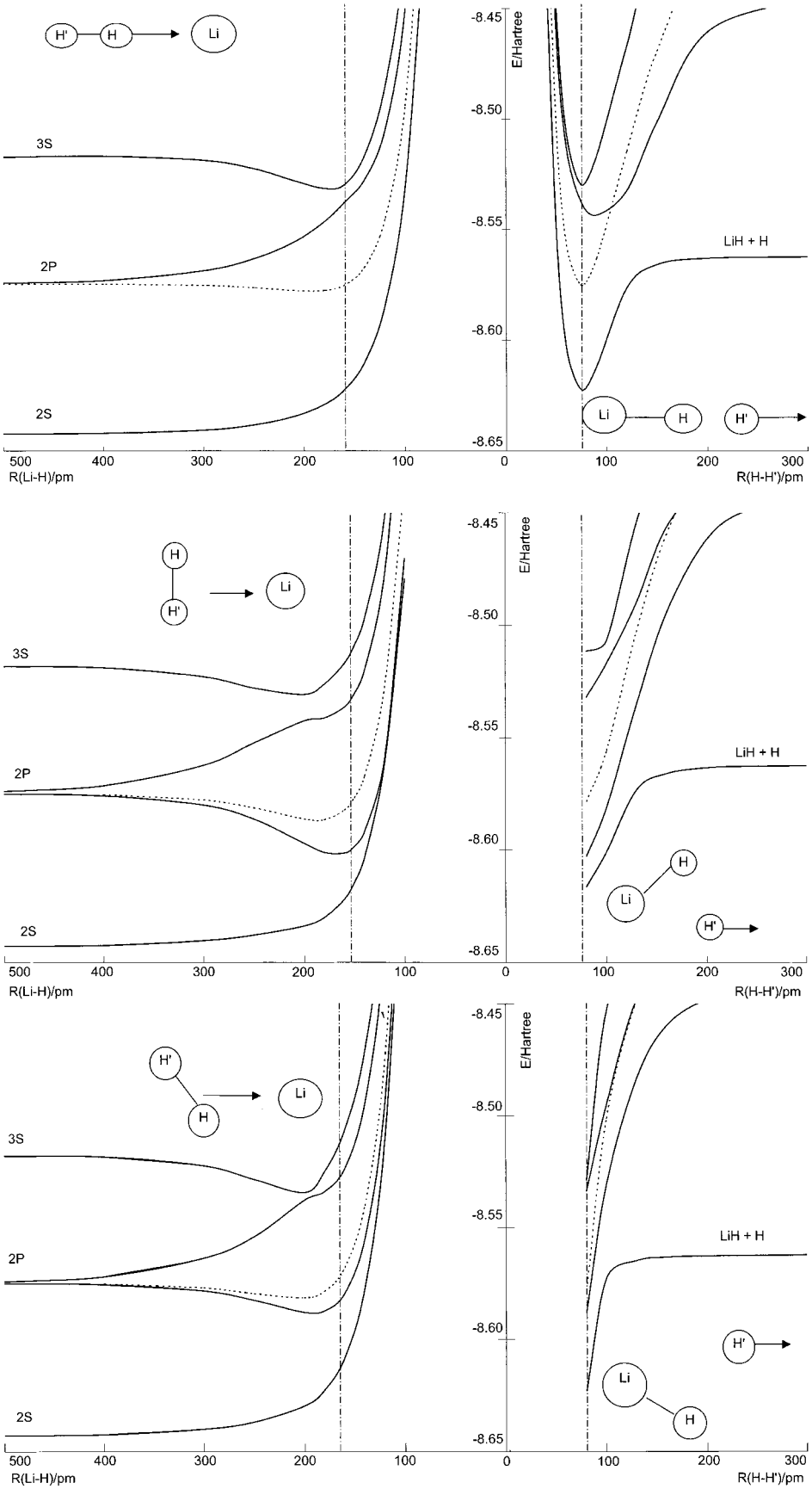

Figure 3. Sections of the potential energy surfaces for the $Li^* + H_2 \rightarrow LiH + H$ reaction (R in pm and E in hartrees). (a, top) Collinear case with $R(H-H') = 75$ pm (left) and with $R(Li-H)=160$ pm (right): the $^2\Sigma^+$ ($^2A'$) states in solid lines and the 2Π (one $^2A''$ and one $^2A'$) states in broken line. (b, middle) Perpendicular (C_{2v}) $Li + H_2$ case with $R(H-H') = 75$ pm (left) and the corresponding $LiH + H$ case (C_s) with $R(Li-H) = 160$ pm (right). (c, bottom) Oblique (C_s) $Li + H_2$ case with $R(H-H) = 75$ pm where the H−H axis makes an angle of 45° with the line joining Li and the center of H_2 (left) and the corresponding $LiH + H$ case (C_s) with $R(Li-H) = 160$ pm (right). In (b) and (c), solid lines are for the $^2A'$ states and broken lines are for the $^2A''$ state. Chained vertical lines represent geometrical form with $R(Li-H) = 160$ pm and $R(H-H') = 75$ pm.

of this $(LiH_2)^*$ intermediate made from the Li(3s) atoms would depend on the initial kinetic energy: if the initial kinetic energy is very low, the elastic collsion may be the predominant process.

One $^2A'$ state coming from the Li(2p) initial state and another $^2A'$ state coming from the Li(3s) state undergo avoided crossing which result in the 3 and the 4 $^2A'$ states. The origin of this interaction can be found from an attraction of the Li(3s) + H_2 and a strong repulsion of the Li($2p_\sigma$) + H_2 near the avoided-crossing region. At less compact geometries, the Li(3s) + H_2 is higher than the Li(2p) + H_2 while the reverse is true at more compact geometries. The smallest energy difference between the 3 $^2A'$ and the 4 $^2A'$ states is less than 280 cm^{-1} and it is found in a C_{2v} case with R(Li−H) = 207 pm and R(H−H′) = 120 pm. (In C_{2v} geometry, both states belong to the A_1 point-group symmetry.) The internal vibration then allows the passage from one potential surface to the other through a diabatic coupling. A transition from the 4 $^2A'$ state to the 3 $^2A'$ state (and vice versa) is estimated to be a fairly probable process so that a nonreactive quenching from 3s to 2p can occur. The energy conservation for this process requires a large increase of the recoil (kinetic) energy of Li and H_2. The vibrational excitation of the hydrogen molecule is also a likely result. The further surface hopping from the 3 $^2A'$ state to the 2 and 1 $^2A'$ states is improbable because the PESs of the lowest two states are too far from the PES of the 3 $^2A'$ state to make quantum tunneling likely.

The 4 $^2A'$ PES originating from Li(3s) has a long distance energy barrier. It is directly connected to the undulating wave function of the Li(3s) AO which has two nodal spheres. The undulating nature of the potential energy in the diatomic molecules of alkali atom has been recently reported.[14] That work has shown that the multiple barriers and multiple potential wells should exist in all electronic states made from an open-shell Rydberg AO and a compact enough closed-shell atom or molecule. In the Li(3s) + H_2 collision, the energy barrier appears to be the highest in collinear case. Several sections of the PES near this energy pass in the collinear case are plotted in Figure 4. The lowest energy pass in the 4 $^2A'$ PES is found for a C_{2v} geometry with R(H−H) = 74.4 pm and R(Li−H) = 515.4 pm with a height of 142 cm^{-1}. In principle, a single energy barrier should exist at long range for the PES originating from the Na-(4s), K(5s), Rb(6s), or Cs(7s) and the hydrogen molecule. Double energy barriers should exist at long range for the PES originating from the Li(4s), Na(5s), K(6s), Rb(7s), or Cs(8s) and the hydrogen molecule, and so forth. The same type of barriers and potential wells can be expected from the np and nd AOs for collinear collision. For coplanar (or bent) cases however, the intermixing between the two (np) or three (nd) components belonging to the a′ irreducible representation (irrep) makes attractive and repulsive PES as can be seen in the Li-(2p) case (see further), which may destroy the undulating energy surfaces. The presence of the energy barrier can be detected by doing a low kinetic energy collision experiment.

In summary, the Li(3s) + H_2 → LiH + H reaction would be a very improbable process. Instead, an electronic quenching, Li(3s) + H_2 → Li(2p) + H_2, with a high translational recoil energy and a high rovibrational excitation of the hydrogen molecule is a likely process. Another process is an inelastic scattering with transfer of the collision energy into the rovibrational energy of the hydrogen molecule, Li(3s) + $H_2(v',J')$ → Li(3s) + $H_2(v'',J'')$ with as much less recoil energy.

(b) Li(2p) + H_2. The Li(2p) initial state which is triply degenerate (not counting the electron spin degree of freedom, i.e., the spin−orbit effect which is negligiblly small) leads to two attractive PESs (2 $^2A'$ and 1 $^2A''$) and a repulsive surface (3 $^2A'$). The 3 and 2 $^2A'$ states are essentially made from the two AOs which have the maximum amplitudes in the molecular plane. They transform to the A_1 irrep and the B_2 irrep in C_{2v} geometry, respectively. The 1 $^2A''$ state is made from the out-of-plane 2p AO and transforms to the B_1 irrep in C_{2v} geometry. The 1 $^2A''$ and 2 $^2A'$ states transform to the $^2\Pi$ irrep in $C_{\infty v}$ geometry, while the 3 $^2A'$ state transforms to the 2 $^2\Sigma^+$ irrep. The 2 $^2A'$ state has a deeper well (6780 cm^{-1}) than that (2845 cm^{-1}) of the 1 $^2A''$ state (Table 2). Considering these binding energies with the zero vibrational energy of the H_2, 2181 cm^{-1}, we may infer that these two states would contain several internal vibrational states. The lowest energy of the 2 $^2A'$ state corresponds to a C_{2v} geometry with the R(Li−H) = 170 pm and R(H−H) = 83 pm (here the H−H distance is significantly elongated in comparison with the free hydrogen molecule). A low kinetic energy collision between a Li(2p) atom and a hydrogen molecule can thus result in a nonreactive scattering through the repulsive (3 $^2A'$) state, or it can result in one of the two stable intermediates (2 $^2A'$ or 1 $^2A''$). The 1 $^2A''$ state cannot

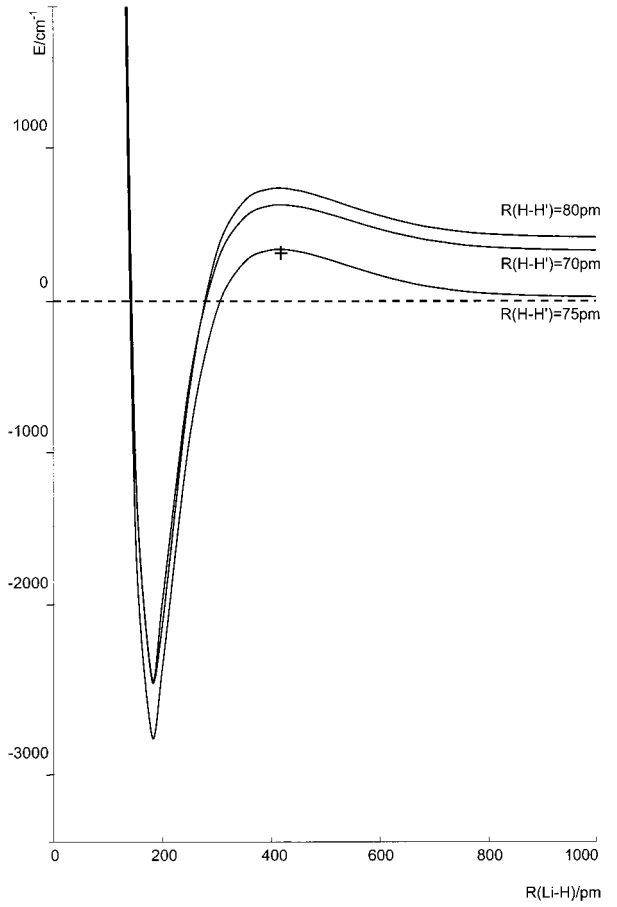

Figure 4. Some collinear sections of the 4 $^2A'$ PES for Li(3s) + H_2 showing the potential barrier.

TABLE 2: Calculated Spectroscopic Data for the LiH_2 Intermediates: Point-Group Symmetry, Equilibrium Internuclear Distances, and the Adiabatic Dissociation Energy (DE)[a]

state	symmetry	R(Li−H)	R(Li−H′)	R(H−H′)	DE
4 $^2A'$	C_s (A′)	175	229	78	3515[b]
1 $^2A''$	C_{2v} (B_1)	188	188	75	2845[c]
2 $^2A'$	C_{2v} (B_2)	170	170	83	6780[c]

[a] Energy in cm^{-1} and R in pm. [b] With respect to Li(3s) + H_2. [c] With respect to Li(2p) + H_2.

proceed to the LiH($X\ ^1\Sigma_g^+$) + H reaction because it is symmetry forbidden. If the initial kinetic energy is high enough to overcome the energy difference between the zero-point energy of LiH + H and that of the Li + H_2, i.e., 1624 cm^{-1}, the LiH can be produced via a PES hopping using the diabatic coupling as in the Li(3s) case.

The 2 and 1 $^2A'$ states lie very close to each other in a compact geometry. In C_s geometry, the potential energy surfaces of these two states cannot cross each other (avoided crossing). However, they belong to two different irreps in C_{2v} geometry, and the crossing is allowed. The accidental crossing between these two potential energy surfaces can be seen in a figure reported by Rossi and Pascale,[3] although they did not mention this crossing at all. In their work, R(H−H) was fixed to 1.4 bohr (74 pm) all along their calculations, and the crossing point seems to be around 160 pm. Martinez's work[4] reported the crossing geometry at R(Li−H) = 151 pm and R(H−H) = 94 pm. Our result shows that the 2 and 1 $^2A'$ states indeed cross in C_{2v} geometry. In fact, the crossing points form a line segment ("seam") when one considers two geometrical parameters, R(Li−H) and R(H−H). The lowest (in terms of the potential energy) crossing point occurs for R(Li−H) = 157 pm and R(H−H) = 90 pm. In this geometry, the potential energy is 6065 cm^{-1} lower than the Li(2p) + H_2 energy disregarding the zero-vibrational energy (G_0) of the hydrogen molecule. This accidental degeneracy was often referred to as a conical intersection by some authors (see ref 13 for instance). However, this accidental degeneracy should be distinguished from the inherent degeneracy originating from the degenerate irrep. The 2 $^2A'$ and the 1 $^2A''$ states become degenerate for the collinear ($C_{\infty v}$) geometry as was mentioned before. Another example of the inherently degenerate case is the much studied ground state problem of the alkali trimers (A_3). Nevertheless, the geometry around this seam line causes a large probability of crossing from one surface to the other. This process has been studied by Martinez[4] by using a multiple spawning technique to describe a semiclassical nuclear dynamics. He showed how the Li(2p) + H_2 collision results mostly in inelastic scattering and partially in reactive scattering. Although the PESs used in that work have been obtained by a rather approximate quantum chemical calculation (effective core potential for the $1s^2$ electrons; no core−valence correlation; double-ζ basis), we think that his result presents a qualitatively valid picture. A quantitative estimation for the cross section would need more refined dynamics calculations.

Li(2p) is certainly a better candidate than Li(3s) or higher states for the photochemical reaction, Li*+ H_2 → LiH + H. The reaction involves a stable C_{2v} intermediate (2 $^2A'$) where the initial collision energy would be redistributed into the internal vibrations before the Li−H bond is formed and the H−H bond is broken. As the surface crossing point lies lower than the Li(2p) + H_2 (hence no reaction barrier), the required kinetic energy is just the endothermicity (1624 cm^{-1}) of the reaction. The other intermediate (1 $^2A''$) cannot participate in the reaction process because the diabatic passage from A″ to A′ is symmetry forbidden. The transition dipole moment for the 1 $^2A''$ ↔ 2 $^2A'$ and 1 $^2A''$ ↔ 1 $^2A'$ transitions for a compact C_{2v} geometry with R(Li−H) = 160 pm and R(H−H) = 75 pm are 0.0096 and 0.3678 D, respectively (where the moment vector is perpendicular to the molecular plane; 1 au = 2.5417 D). If one takes into account that the spontaneous emission is proportional to ΔE^3 or that induced transition is proportional to ΔE^2, the intensity of the former transition is negligible before the latter transition. The transition dipole moment at the same geometry for the 2−1 $^2A'$ transition is much larger (4.6742 D, where the moment vector is aligned to the symmetry axis).

There occurs a partial electron transfer from the lithium atom to the hydrogen atoms during the collision. The degree of the transfer and the charge distribution between the two hydrogen atoms differ from state to state and from one geometry to another. However, the electron transfer from Li to H_2 remains very small in all geometrical approaches during the collision. The electron population along the C_{2v} reaction path and the consecutive center-of-mass conserving product path is analyzed in Figure 5. As the distance between the lithium atom and the hydrogen molecules becomes small following the C_{2v} reaction path on the ground (left part of Figure 5a) or the first excited state (left part of Figure 5b), there occurs a negligible (less than 0.1) electron transfer from the lithium atom to the hydrogen molecule (Figure 5a) or from the hydrogen molecule to the lithium atom (Figure 5b). When a hydrogen atom is progressively detached from the LiH_2 complex following the product path (right part of Figure 5b), the dissociating terminal hydrogen atom (H′) donates the surplus electron population to the companion hydrogen atom (H) to finally form the ground state of the LiH molecule which is ionic (Li^+H^-) near the equilibrium bond distance.

(c) LiH + H → Li* + H_2. The ground state PES shows a downhill descending shape from the initial state, LiH + H, to the final state, Li + H_2. So if one considers only the ground PES, the reaction 3 would be highly efficient. However, the reaction cannot be a single-step process because of the close diabatic coupling between the 1 and 2 A′ states. The following nonradiative unit processes can be considered where the 1 $^2A'$ intermediate can play an important role.

$$LiH(X) + H \rightarrow LiH_2(1\ ^2A') \rightarrow Li(2s) + H_2 \quad (6)$$

$$LiH(X) + H \rightarrow LiH_2(1\ ^2A') \rightarrow LiH_2(2\ ^2A') \quad (7)$$

$$LiH_2(2\ ^2A') \rightarrow Li(2p) + H_2 \quad (8)$$

$$LiH_2(2\ ^2A') \rightarrow LiH_2(1\ ^2A') \rightarrow Li(2s) + H_2 \quad (9)$$

(6) and (8) are adiabatic processes and (7) and (9) involve a surface hopping by diabatic coupling. One should also consider radiative dissociation processes:

$$LiH_2(2\ ^2A') \rightarrow LiH_2(1\ ^2A') + \hbar\omega \rightarrow Li(2s) + H_2 \quad (10)$$

Another radiative transition, $LiH_2(2\ ^2A') \rightarrow LiH_2(1\ ^2A'') + \hbar\omega'$, accompanying an infrared bound-to-bound emission can be neglected in comparison with the radiative transition (10) accompanying a visible bound-to-continuum diffuse-band emission because of the reason explained above. As a consequence, only the 2 $^2A'$ intemediate must be involved in this reaction while both 1 $^2A''$ and 2 $^2A'$ intermediates can be made in the Li(2p) + H_2 reaction. Spectrometric characterization of the two intermediates would contribute much in understanding both reactions.

IV. Discussion

(a) Intermediates. Although the ground state is unstable, the excited states of LiH_2 complex include many stable intermediates. Our work has shown that to each excited state of lithium atom corresponds at least one stable intermediate state with the hydrogen molecule. Our result for the Li(3p) and Li(3d), which we did not discuss here in detail, also showed stable intermedi-

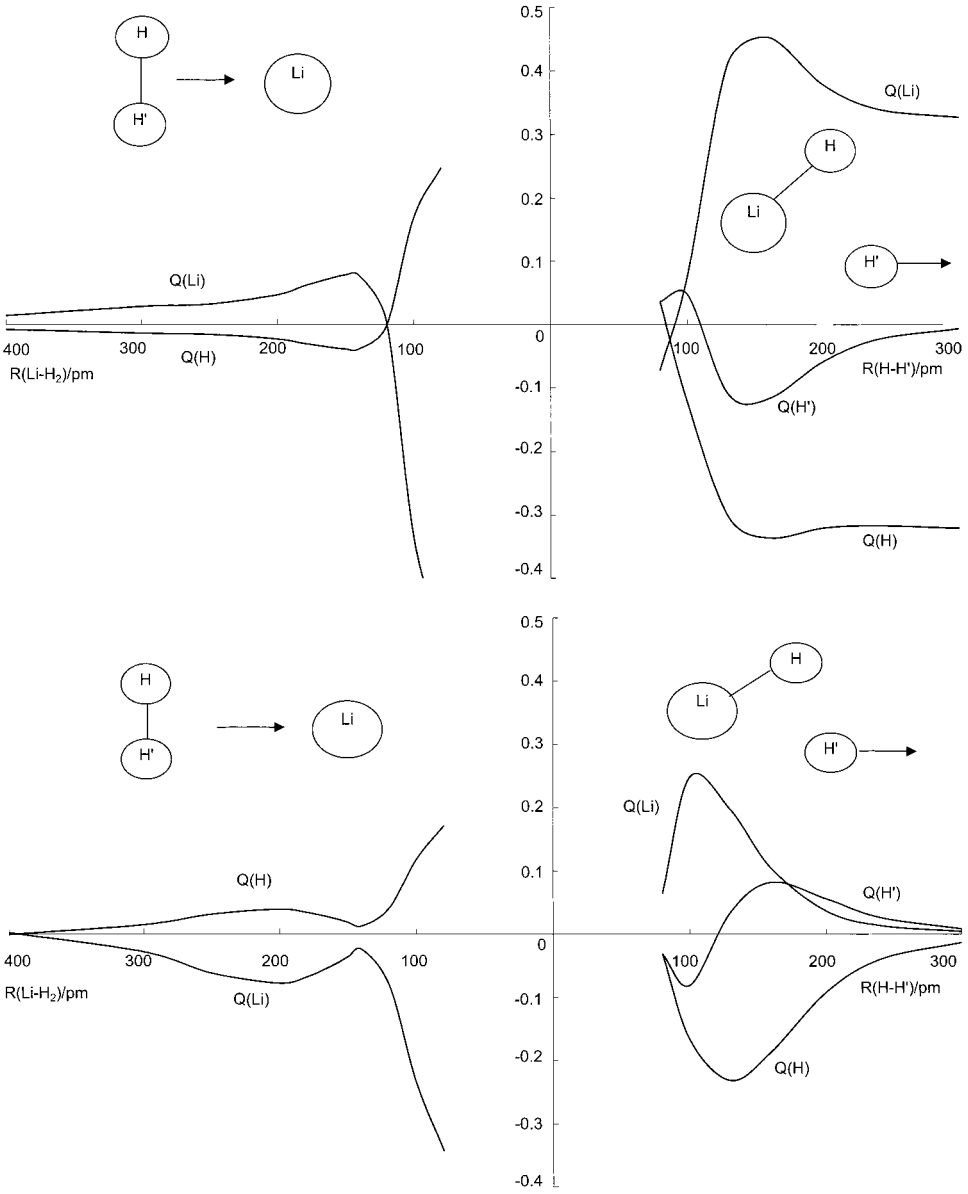

Figure 5. Electron populations of the perpendicular case (a C_{2v} entrant and a C_s departing) as a function of R: (a, top) the 1 $^2A'$ state; (b, bottom) the 2 $^2A'$ state.

ates. This situation is analogous to the diatomic molecules of alkali atom and rare-gas atom, where most of the excited states have stable potential wells.[14] The existence of stable intermediates of the alkali−hydrogen molecule complex has been found by quantum chemical calculations.[16−19] The Na(4p)H_2 intermediate has been observed by Bililign et al.[20] and the K(5p)H_2 intermediate has been observed by Wong et al.[21] in half-collision experiments. From a heat-pipe experiment for the K(7s) + H_2 reaction, Lin and Chang[22] have concluded a single-collision without an intermediate, while a later experiment by Liu and Lin[22,23] for the K(5p−7p) + H_2 reaction supposed an intermediate. An effective core potential calculation for the CsH_2 system has shown all PESs be replusive,[24] thus suggesting no intermediate. A molecular beam experiment by L'Hermite et al.[25] for the Cs(7p, 6d) + H_2 reaction gave no definite answer for the prescence or not of the intermediate (see below). However, a model calculation by L'Hermite[26] showed intermediates.

The existence of the intermediate is crucial for the PES hopping. A single collision is rarely efficient enough for a diabatic transition. The potential well of the intermediate state confines the reactants to a compact geometry for a relatively long lifetime so that many vibrations facilitate a state transition. The transition probability from one PES to another in a single collision is proportional to $P(1 - P)$ where P is a single PES crossing probability. So the maximun transition occurs for $P = {}^1/_2$. In the 1 and 2 $^2A'$ case, P is estimated to be large (i.e. close to 1) when a simple Landau−Zener−Stuckelberg model for diatomic molecules is used for Li−H_2, so the lifetime of the 2 $^2A'$ state becomes an important factor. Martinez[4] has shown this point in a dynamic simulation where P is about 0.9. The equilibrium geometries of the $(LiH_2)^*$ intermediates with Li = 2p, 3s, 3p, or 3d are not linear but bent (C_{2v} or C_s). In fact, we do not know any reported work giving a firm proof for the linear intermediate of metal−H_2 system. The $(LiH_2)^*$ intermediates may be experimentally observed by laser absorption and fluorescence spectroscopy. The bound levels of the 1 $^2A''$ (2p) and the 2 $^2A'$ (2p) states can be studied by exciting them to the bound levels of the higher states, e.g. 4 $^2A'$ (3s), 5 $^2A'$ (3p), 2 $^2A''$ (3p), 6 $^2A'$ (3d), or 3 $^2A''$ (3d) states, or by detecting LiH_2^+ ions through photoionization. Resolution of the vibrational bands or ionization rates may give valuable information about the geometry and the vibrational motion of these intermediates.

Time-resolved spectroscopy may measure the lifetime of the intermediate. The LiH+H reaction is very interesting in this regard. Indeed, this laserless experiment may show chemiluminescence coming not only from the 671 nm line emission but also from a difuse emission originating from the bound-to-unbound fluorescence (10). Fast modulation technique of the atomic or molecular beam and recording the chemiluminescence could reveal radiative lifetime of the $2\ ^2A'$ intermediate.

The intermediates play important roles in the Na + H_2 as can be seen in theoretical[18,27,28] and an experimental[29] studies. Breckenridge and Umemoto[30] have compared the internal energy distribution of the MgH and MgD resulting from the Mg(^{1}P) + H_2 and Mg(^{1}P) + D_2 reactions. They have concluded that the intermediate would live long enough to redistribute its internal energies, and the (MgD_2)* intermediate has a longer lifetime than the (MgH_2)* intermediate (probably due to the larger reduced mass of the former). A stable (MgH_2)*, made from Mg(3s3p, ^{1}P) has been confirmed later by a calculation by Ou et al.[31] A work by Ohmori et al.[32] on the Hg(6s6p, $^3P_1$) + H_2 also suggested the existence of an intermediate. The collision path leading to these intermediates may evolve during a relatively long rovibrational lifetime before resulting in an inelastic quenching or a reaction.

(b) Reaction Mechanism. One can classify the reaction mechanism between the metal atoms and the hydrogen molecule in three categories. The first one concerns preferentially near-collinear collision. Experimental studies on K + H_2,[22,23] Rb-(5d, 7s) + H_2[33] and Cs + H_2[34] favored the collinear collision (or more precisely near-collinear collision, because the truly collinear collision is statistically improbable) as the most reactive geometric approach. Here the rotational energy distribution of AH follows approximately the statistical distribution of a single temperature close to that of the reservoir. The vibrational distribution of AH varied much upon the initial electronic states. The two products, AH and H, are ejected with a large translational (or recoil) energy.

In the second category belong the Mg* + H_2/D_2 case[30,31,35] and the Na* + H_2/HD/D_2 case[20] where bimodal rotational structures have been observed for both AH and AD (with some differences for the large J between the MgH and MgD, while no such differences were found for the NaH and NaD). This was supposed to result from predominantly side-on attack (C_{2v}) leading to an insertion rather than a collinear (or end-on) attack leading to an abstraction. These works gave detailed analyses for the observed spectra in terms of PESs; the attractiveness of the C_{2v} PES favors a near side-on attack, followed by an insertional substitution, resulting in a high rotational distribution. In contrast, the collinear attack (which has a repulsive surface) followed by an abstractive substitution would result in a low rotational distribution because of the zero impact parameter. Our results show that the quenching process, Li(3s) + H_2 → Li(2p) + H_2, or the reactive process, Li(3s) + H_2 → LiH + H, would belong to this category. The collision would take place mainly through a bent (near C_{2v}) geometry. When the rovibrational energy of the hydrogen molecule is low (as in supersonic molecular beam cases with $v = 0$ and $J = 0$ or 1), the attraction force would align the hydrogen molecule in such a way as to end up with more C_{2v} like collisions.

The Cs*+ H_2 study by L'Hermite et al.[25] belongs to the third category where the ratio of the mean recoil translational energy to the mean rotational energy has been observed constant with a ratio of about 2.3, and the Cs−H vibrational energy was weak. The weak vibrational energy has been attributed to the electron jump ("harpooning") occurring at the interatomic distance only slightly larger than the equilibrium distance (R_e) of CsH. No bimodal rotational structure has been reported, which has been interpreted as either there exists no preferred collisional mode (abstractive or insertional) or the reaction may proceed via a stable intermediate (CsH_2)* complex whose existence although has not been confirmed.

(c) Harpooning Model. The "harpooning" model has been initially proposed for the highly exoergic reaction, A + XY, between the alkali metal atoms (A) and the halogen diatomic molecules (XY) where the reactive cross section is very large.[36] In this model, the metal atom donates one electron to the halogen molecule at long intermolecular distances, $A^+ + XY^-$. The attraction between the positively charged metal atom and the negatively charged halogen molecule makes a large reactive cross section to produce $A^+X^- + Y$. It has long been believed that the same model can explain the reaction between the metal atoms and the hydrogen molecule by many authors. However, the alkali−hydrogen case is very different from the alkali−halogen case. The former is a photochemical reaction involving the excited states (and largely endoergic) while the latter concerns the ground state (and largely exoergic). While the electron affinities of the halogen molecules are positive and large, that of the hydrogen molecule is negative (our calculation gave the electron affinity of the Σ_g^{2-} state $-3390\ cm^{-1}$ and that of the Σ_u^{2+} state $-4600\ cm^{-1}$).

Figure 5 does not support harpooning model for the lithium−hydrogen reaction. Indeed, no charge transfer from the lithium atom to the hydrogen molecule occurs at compact geometry either in the ground state or in the excited state (examine in particular the crossing region between the 1 and $2\ ^2A'$ states, i.e., the left parts of Figure 5,a and b). This reaction is rather similar to the metal−rare-gas diatomic molecules or the interaction between one metal atom and a compactly closed shell in general. The driving force for the complex formation (or the origin of the attractive part of the PES) comes from the adaptation of the metal atomic orbitals to the approaching hydrogen molecule, which reinforces the apparent charge at the lithium and the induced dipole of the hydrogen molecule, as was discussed in above. This interaction is of much shorter range (the two electron distributions should overlap significantly) than the ionic attraction of the harpooning model. Therefore, the reactive cross section should be much smaller than in the alkali−halogen cases. The charge transfer only occurs when a hydrogen atom leaves from the Li−H_2 complex (see the right part of Figure 5a), i.e., posterior to the collision.

The harpooning model has been also considered to be suitable to explain the scission of the H−H bond. The main argument was that the transferred surplus electron occupies the antibonding $1\sigma_u$ MO, thereby weakening the H−H bond, and eventually one hydrogen atom will leave from the complex. However, there is one important fact which makes this argument inadequate. The H_2^- molecule in the Σ_u^{2+} state (the ground state where approximately two electrons are in the bonding $1\sigma_g$ MO and one electron is in the $1\sigma_u$ MO) or the Σ_g^{2+} state (the second lowest state where approximately two electrons are in the bonding $1\sigma_g$ MO and one electron is in the $2\sigma_g$ MO) is strongly bound with respect to the H^- + H, and the equilibrium bond distances of these states differ from that of the hydrogen molecule by less than 1 pm. So, just putting one surplus electron to the hydrogen molecule will not be enough to break the H−H bond. We rather think that wide-amplitude internal vibrations may be the key factor for losing one hydrogen atom from the LiH_2 complex.

V. Conclusion

The Li(2p) + H_2 and LiH($X\ \Sigma_g^{1+}$) + H collision experiments are very interesting because at most only three PESs (excluding a strongly repulsive 3 $^2A'$) are involved, so the reaction mechanism would be the simplest among the alkali−hydrogen reactions. As the alkali atom becomes heavy going from Li to Cs, larger and larger number of the PESs are involved so the reaction mechanism becomes more complex. This has been illustrated in the Cs(7p) + H_2 case,[24] where the electronic states should undergo a long series of change 7p → 5d → 7s → 6p → 6s (13 PESs of which nine $^2A'$ and four $^2A''$; in fact, the large spin−orbit effect in the CsH_2 makes those numbers still larger). As a consequence, a large number of elementary reactions take place,[39] and the reactive cross section becomes small. A recent estimation for the Cs($7P_{1/2}$) + H_2 case[40] has given the total reactive cross section of merely 0.6 Å^2.

Our work has predicted some essential features of two reactions, Li + H_2 and LiH($X\ \Sigma_g^{1+}$) + H, by analyzing the PESs. A very recent experiment by the Orsay group on the Li(3s) + H_2 reaction has failed to detect any trace of the LiH production,[41] which is in agreement with our conclusion. Accurately predicting observables would need reaction dynamical studies from our PESs, which require an accurate quantum mechanical method for the three-body multiple-state cases. We hope that the present work will stimulate experimental and theoretical studies for the metal−hydrogen reactions in both directions, (1) and (3), which can greatly improve understanding the photochemical reactions in general. We are aware of several experimental works on alkali−hydrogen systems doing high-resolution spectroscopic studies using molecular beams some of them combined with the ultracold techniques. Low-energy collision can also check the presence of potential energy barrier coming from the ns atomic states.

One should also check the applicability or not of the harpooning model to the interaction between other metal atoms and the hydrogen molecule. Our work in progress on other metal−hydrogen systems (NaH_2, KH_2, CaH_2) and an alkali−halogen system (LiF_2) is showing a remarkable difference between these: while the harpoonig model applies clearly to the alkali−halogen system, it is not the case for the metal−hydrogen systems. This will be presented in the near future.

Acknowledgment. This work was supported by the Korea Science and Engineering Foundation (KOSEF, 985-0300-006-2), the MOST-FOTD project, and the Centre National de la Recherche Scientifique (CNRS). G.H.J. thanks the KFSTS-KOSEF for Brain-Pool fellowship. H.S.L. thanks the ASCI laboratory for visiting scholarship. Professors Bill Stwalley, Goran Pichler, Wei-Tzou Luh, and King-Chuen Lin are thanked for many helpful discussions. Dr. Raymond Vetter is thanked for kindly reading the manuscript.

References and Notes

(1) Tam, A.; Moe, G.; Happer, W. *Phys. Rev. Lett.* **1975**, *35*, 1630.
(2) Dalgarno, A.; Stancil, P. C.; Lepp, S. *Molecular Processes in the Early Universe*; Proceedings of the Second Oak Ridge Symposium on Atomic and Nuclear Astrophysics; IOP Publishing: 1998; pp 137−143.
(3) Rossi, F.; Pascale, J. *Phys. Rev. A* **1985**, *32*, 2657.
(4) Martinez, T. J. *Chem. Phys. Lett.* **1997**, *272*, 139.
(5) Huber, K. P.; Herzberg, G. *Molecular Spectra and Molecular Structure*; Van Nostrand Reinhold: New York, 1979; Vol. 4.
(6) Moore, C. E. *Atomic Energy Levels*; National Bureau Standards (U.S.), Cir. No. 467; G. P. O.: Washington, DC, 1971; Vol. 1.
(7) Froese-Fischer, C. *The Hartree−Fock Method for Atoms*; Wiley: New York, 1977.
(8) Jeung, G.-H.; Spiegelmann, F.; Daudey, J.-P.; Malrieu, J.-P. *J. Phys. B* **1983**, *16*, 2659.
(9) Radzig, A. A.; Smirnov, B. M. *Reference Data on Atoms, Molecules, and Ions*; Springer: Berlin, 1985; p 131.
(10) A package of ab initio programs written by: Anderson, K.; Blomberg, M. R. A.; Fülscher, M. P.; Karlström, G.; Lindh, R.; Malmqvist, P.-A.; Neogrády, P.; Olsen, J.; Roos, B.; Sadlej, A. J.; Schütz, M.; Seijo, L.; Serrano-Andrés, L.; Siegbahn, P. E. M.; Widmark, P.-O. Lund University: Sweden, 1997.
(11) A package of ab initio programs written by: Werner, H. J.; Knowles, P. J. with contributions from Almlöf, J.; Amos, R. D.; Deegan, M. J. O.; Elbert, S. T.; Hampel, C.; Meyer, W.; Peterson, K.; Pitzer, R.; Stone, A. J.; Taylor, P. R.; Lindh, R., 1996.
(12) Mizutani, K.; Yano, T.; Sekiguchi, A.; Hayashi, K.; Matsumoto, S. *Bull. Chem. Soc. Jpn.* **1984**, *57*, 3368. Toyoma, M.; Uchide, T.; Yasuda, T.; Kasai, T.; Matsumoto, S. *Bull. Chem. Soc. Jpn.* **1989**, *62*, 2781. Matsumoto, S.; Toyoma, M.; Yasuda, Y.; Uchide, T.; Ueno, R. *Chem. Phys. Lett*. **1989**, *157*, 142.
(13) Clarke, N. J.; Sironi, M.; Raimondi, M.; Kumar, S.; Gianturco, F. A.; Buonomo, E.; Cooper, D. L. *Chem. Phys.* **1998**, *233*, 9.
(14) Yiannopoulou, A.; Jeung, G.-H.; Park, S. J.; Lee, H. S.; Lee, Y. S. *Phys. Rev. A*, **1999**, *59*, 1178.
(15) Yarkony, D. R. *Acc. Chem. Res.* **1998**, *31*, 511.
(16) Botschwina, P.; Meyer, W.; Hertel, A. V.; Reiland, W. *J. Chem. Phys*. **1981**, *75*, 5438.
(17) Yarkony, D. *J. Chem. Phys*. **1986**, *84*, 3206. Kryachko, E. S.; Yarkony, D. R. *Theor. Chem. Acc*. **1998**, *100*, 154.
(18) Vivie-Riedle, R.; Hering, P.; Kompa, K. L. *Z. Phys. D* **1990**, *17*, 299.
(19) Hack, M. D.; Truhlar, D. G. *J. Chem. Phys*. **1999**, *110*, 4315.
(20) Bililign, S.; Kleiber, P. D. *Phys. Rev. A* **1990**, *42*, 6938; *J. Chem. Phys.* **1992**, *96*, 213; Bililign, S.; Kleiber, P. D.; Kearney, W. R.; Sando, K. M. *J. Chem. Phys.* **1992**, *96*, 218.
(21) Wong, T.-H.; Kleiber, P. D.; Yang, K.-H. *J. Chem. Phys.* **1999**, *110*, 6743.
(22) Lin, K.-C.; Chang, H.-C. *J. Chem. Phys.* **1989**, *90*, 6151; Luo, Y. L.; Lin, K. C.; Liu, D. K.; Liu, H. J.; Luh, W. T. *Phys. Rev. A* **1992**, *46*, 3824; Liu, D. K.; Lin, K. C. *J. Chem. Phys.* **1996**, *105*, 9121.
(23) Liu, D. K.; Lin, K. C. *J. Chem. Phys.* **1997**, *107*, 4244.
(24) Lepetit, M. B.; LeDourneuf, M.: Launay, J. M.; Gadéa, F. X. *Chem. Phys. Lett.* **1987**, *135*, 377. Gadéa, F. X.; Spiegelmann, F.; Pélissier, M.; Malrieu, J. P. *J. Chem. Phys.* **1986**, *84*, 4872. Crépin, C.; Picqué, J. L.; Rahmat, G.; Vergès, J.; Vetter, R.; Gadéa, F. X.; Pélissier, M.; Spiegelmann, F.; Malrieu, J. P. *Chem. Phys. Lett.* **1984**, *110*, 395. Gadéa, F. X.; Jeung, G.-H.; Pélissier, M.; Malrieu, J. P.; Picqué, J. L.; Rahmat, G.; Vergès, J.; Vetter, R. *Laser Chem.* **1983**, *2*, 361.
(25) L'Hermite, J.-M.; Rahmat, G.; Vetter, R. *J. Chem. Phys.* **1990**, *93*, 434. L'Hermite, J.-M.; Rahmat, G.; Vetter, R. *J. Chem. Phys.* **1991**, *95*, 334. L'Hermite, J.-M. *J. Chem. Phys.* **1992**, *97*, 6215.
(26) L'Hermite, J.-M., Doctorate Thesis, Université de Paris Sud, Orsay, 1990.
(27) Halvick, P.; Truhlar, D. G. *J. Chem. Phys*. **1992**, *96*, 2895. Tawa, G. J.; Mielke, S. L.; Truhlar, D. G.; Schwenke, D. W. *J. Chem. Phys*. **1994**, *100*, 5751.
(28) Martinez, T. J.; Ben-Nun, M.; Levine, R. D. *J. Phys. Chem*. **1997**, *101*, 6389. Ben-Nun, M.; Martinez, T. J.; Levine, R. D. *J. Phys. Chem*. **1997**, *101*, 7522.
(29) Motzkus, M.; Pichler, G.; Campa, K. L.; Hering, P. *J. Chem. Phys*. **1997**, *106*, 9057.
(30) Breckenridge, W. H.; Umemoto, H. *J. Chem. Phys.* **1984**, *80*, 4168. Breckenridge, W. H.; Jouvet, C.; Soep, B. *J. Chem. Phys.* **1986**, *84*, 1443. Breckenridge, W. H.; Wang, J. H. *Chem. Phys. Lett*. **1987**, *137*, 195.
(31) Ou, W.-R.; Liu, D.-K.; Lin, K.-C. *J. Chem. Phys*. **1998**, *108*, 1475.
(32) Ohmori, K.; Takahashi, T.; Chiba, H.; Saito, K.; Nakamura, T.; Okunishi, M.; Ueda, K.; Sato, Y. *J. Chem. Phys*. **1996**, *105*, 7464; *105*, 7474.
(33) Chen, M.-L.; Lin, W.-C.; Luh, W.-T. *J. Chem. Phys.* **1997**, *106*, 5972. Fan, L.-H.; Chen, J.-J.; Lin, Y.-Y.; Luh, W.-T. *J. Phys. Chem*. **1999**, *103*, 1300.
(34) Huang, X.; Zhao, J.; Xing, G.; Xing, X.; Bersohn, R. *J. Chem. Phys.* **1996**, *104*, 1338.
(35) Lin, K.-C.; Huang, C.-T. *J. Chem. Phys.* **1989**, *91*, 5387.
(36) Ogg, R. A.; Polanyi, M. *Trans. Faraday Soc.* **1935**, *31*, 604. Evans, M. G.; Polanyi, M. *Trans. Faraday Soc*., **1938**, *34*, 11. Magee, J. L. *J. Chem. Phys*., **1940**, *8*, 687. Hershbach, D. R. In *Molecular Beams*; Ross, J., Ed.; Wiley-Interscience: New York, 1966; Chapter 9.
(37) Eyler, E. E.; Melikechi, N. *Phys. Rev. A* **1993**, *48*, R18.
(38) Stwalley, W. C.; Zemke, W. T. *J. Phys. Chem. Ref. Data* **1993**, *22*, 87.
(39) Sayer, B.; Ferray, M.; Lozingot, J.; Berlande, J. *J. Chem. Phys.* **1981**, *75*, 3894. Visticot, J. P.; Ferray, M.; Lozingot, J.; Sayer, B. *J. Chem. Phys.* **1983**, *79*, 2839.
(40) Cavero, V.; Rahmat, G.; Vetter, R. *J. Chem. Phys.* **1999**, *110*, 3428.
(41) Cavero-Machado, V. Doctorate Thesis, Université de Paris Sud, Orsay, 1997.